

Simulation of volatile gas release from a small dry wood particle undergoing pyrolysis in a hot convective flow field

Ulf Sand*, Jan Sandberg*, Rebei Bel Fdhila**

* Department of Public Technology, Fluid Dynamics Research Group, Mälardalen University, Box 883, SE - 721 23, Västerås, Sweden

** ABB, Corporate Research, Dept. AT, Forsgränd 7, SE - 721 78, Västerås, Sweden & Department of Public Technology, Fluid Dynamics Research Group, Mälardalen University, Box 883, SE - 721 23, Västerås, Sweden

Abstract

A two step reaction model for the pyrolysis process of a dry cylindrical pine wood particle, exposed to a hot gas flow field, has been developed adding user defined subroutines to the commercial computational fluid dynamics code CFX 4.4. The wood particle is fixed in space and has a diameter of 15.0 mm and a height of 60.0 mm. The particle temperature is initially 30 °C when it is introduced to the 500 °C hot flow. The surrounding walls have a constant temperature of 500 °C. The simulation results have been compared with the experimental data of Pyle and Zaror (1984).

The furnace is cylindrical as well as the wood particle which is fixed on the axis of symmetry. The computational domain is axisymmetric. The laminar flow around the particle, and the flow inside the porous wood, are fully coupled, allowing the release of volatile pyrolysis gas from the wood to mix with the surrounding flow field. The transport and the production of char, tar and pyrolysis gas and the consumption of wood, is calculated. The model includes convective, conductive and radiation heat transfer modes in axial and radial direction.

Results from the simulation runs show the temperature profiles in the wood, the overall reduction of mass due to conversion of the wood during the heating, the plumes of concentration of volatile pyrolysis gas released from the particle surface as well as vector plots of the velocity of the pyrolysis gas plumes.

Introduction

The purpose of this work is to see if it is possible to achieve a two dimensional CFD model that can simulate the release of volatile gas from a wooden chip fixed in space where both the inner structure and the surface of the porous wood structure as well as the surrounding gaseous atmosphere is included. The modelled chip is in this case chosen to be cylindrical with a diameter of 15.0 mm and a height of 60.0 mm.

Earlier work on the topic of wood pyrolysis by the authors Sand, Sandberg and Bel Fdhila resulted in the implementation of a CFD model for the pyrolysis of a birch wood log. The aim of that work was to achieve a model to be compared to and validated against the experimental work of Larfeldt (2000). The model was built and simulated using as many of the known thermodynamic and transport properties as possible and included both the porous structure of the wood log as well as the surrounding gas.

The comparison between the data from simulations and the measurements of Larfeldt (2000) where mainly concerning temperature profiles, at different radial positions in the wood log, and also the reduction of the overall mass of the wood log during pyrolysis for dry and moist wood. The comparison show good agreement between data from the simulations and the measurements.

The work at hand is therefore to be regarded as an extension of the earlier work mentioned, however now focusing on the distribution of the concentration and the speed of the released volatile matter from the pyrolysis out of the cylindrical wood chip.

The results from the present simulations give a qualitative estimate of the solid centre temperature and the pyrolysis conversion, by comparison to experimental data from Pyle and Zaror (1984). The simulations also gives a quantitative picture of the size of the plumes of concentration of released volatile gas penetrating the surrounding gas. The gas plumes acts mainly from the top and bottom end of the wood cylinder. The model calculates the velocity components of these plumes in order to give an estimate of the speed by which the volatile gas is released.

In the following presentation the axisymmetrical flow domain has been divided in two categories: one is the more or less porous wooden log where the transport is governed by diffusion and in some special cases laminar convection. The other region is the turbulent, or in this case laminar, gas surrounding the wood log. Since these regions are governed by slightly different equations it is important to maintain all physical aspects, consistently, between the two regions.

A detailed description of the governing equations for the flow, the heat and the species transport as well as the mechanisms of conversion from virgin dry wood to the yield of char, tar and gas are presented.

Mathematical model

The computational domain

The axisymmetrical computational grid with the region of the wood and grid boundaries are depicted below. The grid consists of 230 vertical and 50 horizontal volume cells thus resolving every millimetre in the axial direction and every half millimetre in the radial direction of the physical domain.

During the simulation the gas inlet velocity is specified to 0.0 m/s. By applying this boundary condition, any resulting velocities, higher than zero, is a consequence of the migration of the pyrolysis gasses leaving the wood cylinder. The pressure is specified to 1atm at the outlet boundary and the temperature is specified to 500 °C at the walls and the inlet boundary.

Even though the simulation is transient, the boundary conditions stated above are assumed to be constant over time, which roughly was the case in the experiments of Pyle and Zaror (1984). The initial temperature of the wood log is 30 °C and the surrounding gas temperature is 500 °C.

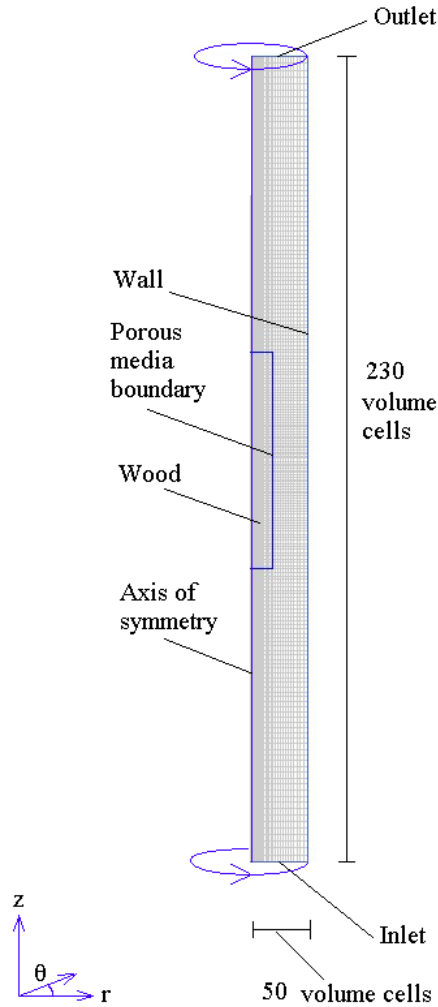


Figure 1: The computational 2-D axisymmetrical domain.

Modelled species

The species, confined to the porous structure of the wooden cylindrical chip, are assumed to be; wood, char and tar. The dominant gaseous pyrolysis species leaving the wood log or flowing in the free stream in the case of pyrolysis, with or without combustion, are typically; O_2 , CO_2 , CO , H_2O , N_2 , H_2 , CH_4 , NH_3 , HCN and NO . However in this model all these gaseous species are compounded into one model specie, namely gas. This results in a set of four model species; **wood**, **char**, **tar** and **gas**.

Chemical mechanisms for the pyrolysis of wood

There are numerous articles, varying in the degree of details, available on the reaction mechanisms and reaction rates of pyrolysis for different types biomass fuels. Some models are simply made of a one step mechanism from the fuel at hand to the yield or yields of the pyrolysis. One of the more sophisticated ways to model the pyrolysis of wood is to apply a mechanism of two steps, a primary and a secondary pyrolysis step, as presented by Di Blasi (1996):



Where the rates of conversion due to pyrolysis are:

| | | | | | | |
|-------------------------------|---|-------|---------------------|-----------------------|---------|---------------------------|
| Wood $\xrightarrow{k_1}$ Gas | $k_1 = 1.52E7 \exp\left(-\frac{139.2}{RT}\right)$ | [1/s] | Font et al. (1990) | $\Delta h_1 = -418.0$ | [kJ/kg] | Chan et al. (1985) |
| Wood $\xrightarrow{k_2}$ Tar | $k_2 = 5.85E6 \exp\left(-\frac{119}{RT}\right)$ | [1/s] | Font et al. (1990) | $\Delta h_2 = -418.0$ | [kJ/kg] | Chan et al. (1985) |
| Wood $\xrightarrow{k_3}$ Char | $k_3 = 2.98E3 \exp\left(-\frac{73.1}{RT}\right)$ | [1/s] | Font et al. (1990) | $\Delta h_3 = -418.0$ | [kJ/kg] | Chan et al. (1985) |
| Tar $\xrightarrow{k_4}$ Gas | $k_4 = 2.6E6 \exp\left(-\frac{108}{RT}\right)$ | [1/s] | Liden et al. (1988) | $\Delta h_4 = 42.0$ | [kJ/kg] | Koufopoulos et al. (1991) |
| Tar $\xrightarrow{k_5}$ Char | $k_5 = 1.0E6 \exp\left(-\frac{108}{RT}\right)$ | [1/s] | Di Blasi (1993a) | $\Delta h_5 = 42.0$ | [kJ/kg] | Koufopoulos et al. (1991) |

Model equations for the inner of the wood log

Since we in this work only consider the flow inside the particle to be laminar, the Navier-Stokes equations for a porous media is applied for the wood log. The transport equations in this text are written in a general manner but the actual code used in the simulations is two dimensional, i.e. in the axisymmetrical coordinate system (r,z) . The reason for this is simply to speed up the calculation procedure and this is allowable if it is assumed that the boundary layer on the surface area is uniformly distributed over the cylindrical wood log circumferential angle, θ , and that the free gas flow movement is not governed by large three dimensional eddies. Since the flow in these simulations is supposed to be laminar and all variations over θ are close to zero, the assumption above is valid.

Continuity

$$\frac{\partial}{\partial t} \gamma \rho + \nabla \cdot (\rho \mathbf{K} \cdot \mathbf{U}) = 0 \quad (1)$$

Momentum

$$\frac{\partial}{\partial t} (\gamma \rho \mathbf{U}) + \nabla \cdot (\rho (\mathbf{K} \cdot \mathbf{U}) \otimes \mathbf{U}) - \nabla \cdot (\mu \mathbf{K} \cdot (\nabla \mathbf{U} + (\nabla \mathbf{U})^T)) = -\gamma \mathbf{R} \cdot \mathbf{U} - \gamma \nabla p \quad (2)$$

where γ is the volume porosity and $\mathbf{K} = (K^{ij})$ is the area porosity tensor, which is a symmetric second rank tensor. μ is the viscosity and $\mathbf{R} = (R^{ij})$ is the resistance to flow in the porous medium.

Multi-component equation of state

The density of the solid wood/char log was calculated according to the multi-component equation of state:

$$\frac{1}{\rho} = \sum_{\alpha=1}^{N_{\text{species}}} \frac{Y_{\alpha}}{\rho_{\alpha}} \quad \text{Where } Y_{\alpha} \text{ is the mass-fraction of species } \alpha$$

$$Y_{\alpha} = \frac{m_{\alpha}}{\sum_{\alpha} m_{\alpha}} \quad \text{and} \quad \sum_{\alpha}^{N_{\text{species}}} Y_{\alpha} = 1$$

In the simulations however, only the heavy species were included, meaning wood and char, yielding:

$$\frac{1}{\rho} = \frac{Y_{\text{wood}}}{\rho_{\text{wood}}} + \frac{Y_{\text{char}}}{\rho_{\text{char}}}$$

This can be written in terms of the species volume fractions, r , giving:

$$\rho = r_{wood} \rho_{wood} + r_{char} \rho_{char} \quad (3)$$

Species transport

$$\frac{\partial}{\partial t} (\gamma \rho Y_\alpha) + \nabla \cdot (\rho \mathbf{K} \cdot \mathbf{U} Y_\alpha) - \nabla \cdot (\Gamma_\alpha \mathbf{K} \cdot \nabla Y_\alpha) = -\gamma S_\alpha \quad (4)$$

Γ_α is the diffusion constant, $\Gamma_\alpha = \rho D_{\alpha\beta}$, which may be different between different species and different directions. There is one transport equation for every species and the effect of the variety of the different species density on the multi-component mixture will be captured by the multi-component equation of state. S_α is the source or sink term for the conversion between the different species, due to pyrolysis.

Using the mentioned two-step pyrolysis mechanism of Di Blasi (1996), this expands into the following set of sink/source terms to be applied:

$$S_{WOOD} = -k_1 Y_{WOOD} - k_2 Y_{WOOD} - k_3 Y_{WOOD}$$

$$S_{CHAR} = k_1 Y_{WOOD} + k_5 Y_{TAR}$$

$$S_{TAR} = k_2 Y_{WOOD} - k_4 Y_{TAR} - k_5 Y_{TAR}$$

$$S_{GAS} = k_3 Y_{WOOD} + k_4 Y_{TAR}$$

Energy

$$\frac{\partial}{\partial t} (\gamma \rho H) + \nabla \cdot (\rho \mathbf{K} \cdot \mathbf{U} H) - \nabla \cdot (\Gamma \mathbf{K} \cdot \nabla H) = \gamma Q_{pyrolysis} + \gamma Q_{radiation} \quad (5)$$

where Γ is the thermal diffusivity, $\Gamma = \frac{\lambda}{C_p}$. H is the total enthalpy according to: $H = h + \frac{1}{2} \mathbf{U}^2$, where h is the thermodynamic enthalpy:

$$h = \bar{C}_p(T)T - \bar{C}_p(T_{ref})T_{ref} \quad (6)$$

where \bar{C}_p is defined by:

$$\bar{C}_p(T) = \frac{1}{T} \int_0^T C_p(T') dT' \quad (7)$$

The term, $Q_{pyrolysis}$, is the pyrolysis enthalpy source terms due to the conversion according to the two-step mechanism reaction rates as presented above:

$$Q_{pyrolysis} = \sum_{i=1}^3 k_i \rho_{Solid} Y_{WOOD} \Delta h_i + \sum_{i=4}^5 k_i \rho_{Solid} Y_{TAR} \Delta h_i \quad [\text{kJ/s m}^3] \quad (8)$$

Thermal radiation

In this work, the radiative mode of heat transfer is considered only to take place between the furnace walls and the surface area of the wood cylinder, thus neglecting the radiative aspects of the gas surrounding the wood cylinder. The wall and the wood surfaces are regarded as being diffuse and gray. Each of the volume cells on the outer boundary surface of the wood cylinder are treated as small convex object in a large cylindrical cavity, the cavity being the furnace vessel itself. Using this approximate assumption, the radiative heat transfer from the furnace walls on a single volume cell can be calculated by:

$$Q_{radiation} = \frac{\tilde{\sigma} A_{wood\ cell} (T_{wall}^4 - T_{wood\ cell}^4)}{\frac{1}{\tilde{\epsilon}_{solid}} + \frac{(1 - \tilde{\epsilon}_{wall}) d_{wood}}{\tilde{\epsilon}_{wall} d_{wall}}} \quad (9)$$

Where $d_{wood} = 0.015$ [m] and $d_{wall} = 0.05$ [m] are the diameters of the wood cylinder and the furnace, respectively.

Since the initial wood cylinder temperature is approximately 30 °C when it is introduced in the hot furnace environment, with a gas and wall temperature of 500 °C, the radiative heat transfer is directed from the walls to the wood surface.

The emissivity of the wood log changes as the wood is converted to char. As a consequence of this the effective emissivity, $\tilde{\epsilon}_{solid}$, of the log has to be modelled. In the simulations the following simple model is used, giving a simple linear weighting of the emissivity by the mass fractions of wood and char:

$$\tilde{\epsilon}_{solid} = \tilde{\epsilon}_{Wood} Y_{Wood} + \tilde{\epsilon}_{Char} Y_{Char} \quad (10)$$

Thermal conductivity in the wood log

The pyrolysis process effects both the physical and the thermodynamical properties of the wood. The thermal conductivity of wood undergoing pyrolysis is altered in many ways since; it changes with the temperature in the wood, it changes due to the conversion from wood to char and gas and it changes with various changes in the physical structure of the wood, such as changes in pore size and by the creation of cracks.

The thermal conductivity, used in the simulations is given by:

$$\lambda_{eff} = \xi \lambda_{\parallel} + (1 - \xi) \lambda_{\perp} \quad (11)$$

Where λ_{\parallel} is the effective thermal conductivity in the direction parallel to the wood grains and λ_{\perp} in the direction perpendicular to the grains. The so called bridge factor, ξ , is introduced to simulate the real porous material arrangement. If the heat conduction is parallel to the wood grains, the bridge factor from literature, Grönli (1996), varies between 0.8 and 1.0 and if the heating is perpendicular to the grains, the bridge factor varies between 0.35 and 0.6. The thermal conductivity parallel and perpendicular to the wood grains are given by:

$$\lambda_{\parallel} = \sum_{\alpha=1}^{N_{species}} r_{\alpha} \lambda_{\alpha} \quad \text{and} \quad \lambda_{\perp} = \frac{1}{\sum_{\alpha=1}^{N_{species}} \frac{r_{\alpha}}{\lambda_{\alpha}}}$$

Where r_{α} is the volume fraction of species α . This approach is anisotropic since the effective conductivity parallel and perpendicular to the wood grains are not the same. In this work however, the thermal conduction is assumed to be mostly perpendicular to the wood grains. Therefore a isotropic model involving only the perpendicular bridge factor is used. The perpendicular bridge factor used is 0.35 for the dry wood.

In the simulations only the heavy species in the wood are included in the calculation of the thermal conductivity, meaning wood and char:

$$\lambda_{\parallel} = r_{wood} \lambda_{wood} + r_{char} \lambda_{char} \quad (12) \quad \text{and} \quad \lambda_{\perp} = \frac{1}{\frac{r_{wood}}{\lambda_{wood}} + \frac{r_{char}}{\lambda_{char}}} \quad (13)$$

Specific heat

The discontinuity in specific heat, created by the sharp change in species composition, when moving from the solid wood through the wood outer boundary and into the gaseous surrounding atmosphere, creates solutions with unphysical temperature oscillations. The reason for this is due to the fact that the energy equation is written in terms of enthalpy and not in terms of temperature in CFX 4.4.

To overcome this problem a weighted constant average specific heat was applied to all chemical species, according to:

$$\tilde{C}_p = \frac{\sum_{\alpha=1}^{N_{species}} Y_{\alpha} \rho_{\alpha} C_{p,\alpha}}{\sum_{\alpha=1}^{N_{species}} Y_{\alpha} \rho_{\alpha}}$$

The density of each specie was then adjusted so that the thermal diffusivity of each individual specie,

$$\Gamma_{\alpha} = \frac{\lambda_{\alpha}}{\rho_{\alpha} C_{p,\alpha}}, \text{ still holds for the weighted constant average specific heat, } \tilde{C}_p, \text{ meaning:}$$

$$\rho_{\alpha,korr} = \frac{\lambda_{\alpha}}{\Gamma_{\alpha} \tilde{C}_p} \quad (14)$$

The only negative aspect of this approach is that the calculation of the momentum is slightly wrong, however this has little impact on the flow field in these simulations since the surrounding atmosphere is pure gas and the species convection in the wood is almost solemnly governed by the permeability.

Permeability in the wood log

The flow of gas inside the wood log is of course very limited due to the fact that the physical structure of wood consists of a large number of clustered small pores. The pore walls acts as barriers largely preventing convective flows to move from one neighbouring pore to another.

The resistance to internal flow, the permeability, is modelled by the resistance term, \mathbf{R} , in the momentum equation, as:

$$\mathbf{R} = \frac{1}{\kappa}$$

Where κ is the permeability. Data for gas permeability are taken from Larfeldt (2000). Since the wood permeability typically has a very small value, $10.0\text{E-}08 - 10.0\text{E-}18$, the value of the resistance term will be very high, thus acting as a limiter for flow in the porous media momentum equation.

Porosity in the wood log

The area porosity, \mathbf{K} , and the volume porosity, γ , in the porous media governing equations of the wood log, was set equally in the simulations. The volume porosity has the unit of $[m^3]$ and is given by: $\gamma = \varepsilon V_{cell}$.

Where ε is the cell porosity given by the equation:
$$\varepsilon = \frac{\sum_{\alpha=1}^{N_{\text{gaseous species}}} \frac{Y_{\alpha}}{\rho_{\alpha}}}{\sum_{\alpha=1}^{N_{\text{total species}}} \frac{Y_{\alpha}}{\rho_{\alpha}}}$$

However, the initial wood porosity and the char porosity was measured by Larfeldt (2000). The measured value for the porosity of wood and char was 0.68 and 0.9 respectively. In this work the following simple linear model was used to calculate the porosity during the transition from wood to char:

$$\varepsilon = \varepsilon_{\text{initial, wood}} + (1 - Y_{\text{wood}})(\varepsilon_{\text{char}} - \varepsilon_{\text{initial, wood}}) \quad (15)$$

Shrinkage of the wood during pyrolysis

From the measurements of Larfeldt (2000), the radial shrinkage of a birch wood log undergoing rapid heating is in the range of 12 to 28 %. Workers Davidsson and Pettersson (2002) reported a radial shrinkage of 15 to 40 % of a ~ 5 mm birch wood cube. Pyle and Zaror (1984) reported a maximal radial shrinkage of 30 % for pine wood cylinders.

In the present work a somewhat low radial shrinkage of 20 % is assumed for the modelled pine cylinder. This radial shrinkage is then recalculated as a change in cylindrical volume by 36 %. The volumetric shrinkage factor, $\varphi = 0.36$, is then applied on the weighted density calculation in order to give a corrected mass whilst keeping the cell volumes constant.

The shrinkage is strongly coupled by the production of char, thus the density reduction is only applied on the char volume fraction term in the expression for the density:

$$\rho = r_{\text{wood}} \rho_{\text{wood}} + r_{\text{char}} \rho_{\text{char}} (1 - \varphi) \quad (16)$$

Pyle and Zaror (1984) studied the impact the shrinkage has on the heating of a pine wood cylinder by the use of a shrinking grid in their model. As the size of their modelled particle decreases there is a tendency that the rate of heat conduction through the wood is increased, however the shrinkage decreases the external surface of the particle and therefore the total heat flux through the surface diminishes. They found from simulations with these two counteracting effects that the solution only varied by 3 % compared to simulations without any shrinkage at all.

In the present work, by applying the shrinkage factor on the solid density, the decrease of mass in one cell volume due to shrinkage is modelled. Then, in order to keep the thermal diffusivity, $\Gamma = \frac{\lambda}{\rho C_p}$, constant whilst

applying the shrinkage factor on the density, the thermal conductivity also has to be altered by the use of the shrinkage factor on the char volume fraction. The reason for doing this is that by keeping the cell volume constant and only alter the density by the shrinkage factor the external wood surface is much to big and thus the heat flux into the particle will be to high. This counteraction follows the discussion on shrinkage by Pyle and Zaror (1984).

Model equations for solving the convective gas flow surrounding the wood log

Continuity

$$\frac{\partial}{\partial t} \rho + \nabla \cdot (\rho \mathbf{U}) = 0 \quad (17)$$

Momentum

$$\frac{\partial}{\partial t} (\rho \mathbf{U}) + \nabla \cdot (\rho \mathbf{U} \otimes \mathbf{U}) = \mathbf{B} + \nabla \cdot \boldsymbol{\sigma} \quad (18)$$

\mathbf{B} is the gravity body force, which is neglected in this work, and $\boldsymbol{\sigma}$ is the stress tensor: $\boldsymbol{\sigma} = -p\delta + \left(\zeta - \frac{2}{3}\mu\right)\nabla \cdot \mathbf{U}\delta + \mu(\nabla\mathbf{U} + (\nabla\mathbf{U})^T)$

Equation of state

The density of the surrounding fluid is set to the constant value of density of air, $\rho = \rho_{air}$.

Species transport

$$\frac{\partial}{\partial t} (\rho Y_\alpha) + \nabla \cdot (\rho \mathbf{U} Y_\alpha) - \nabla \cdot (\Gamma_\alpha \nabla Y_\alpha) = 0 \quad (19)$$

Energy

Since neither thermal radiation nor pyrolysis is relevant in the surrounding gas, the energy equation is given by:

$$\frac{\partial}{\partial t} (\rho H) + \nabla \cdot (\rho \mathbf{U} H) - \nabla \cdot (\lambda \nabla T) = 0 \quad (20)$$

where λ is the thermal diffusion coefficient. H is the total enthalpy according to: $H = h + \frac{1}{2} \mathbf{U}^2$, where h is the thermodynamic enthalpy given by equation (6).

Simulations

Since this work is focused on the release of the volatiles from the wood to its surroundings it is important to see what impact the velocity and momentum of the plumes of volatile pyrolysis gas has on the surrounding gas velocity field.

One other important aspect is the time needed to fully heat the wood structure to 500 °C. The heating is governing the rate of conversion from wood to char and of course also the reduction of the overall mass of the cylindrical wood chip.

Studied parameters

Wood/char heating

As commented by Pyle and Zaror (1984), the radiation heat transfer accounts for approximately 80 % of the total heat transfer to the wood cylinder surface. Once the heat is transported to the wood surface the thermal conduction and in some cases convection accounts for the internal heating in the wood structure.

The most important factors for the internal heating in the wood cylinder is therefore the thermal conductivity (thermal diffusivity) and the modelling of the convective flow in the different regions of the wood cylinder during the transition from wood to char.

Comparison of the simulated temperature profile in the wood with the measured wood centre temperature from Pyle and Zaror (1984) experiments is presented in order to estimate the validity of the model.

Conversion from wood to char

The simulated conversion from wood to char during the pyrolysis process is compared to the measured conversion by Pyle and Zaror (1984). If the heating of the wood cylinder is modelled correctly, it is possible to assess whether the used pyrolysis reaction rates are adequate or not.

Volatiles released to the surroundings

Both the speed and the mass fraction of the released volatile pyrolysis gas is calculated during the simulations. This makes it possible to estimate the size and the volatile gas concentration of the plumes of pyrolysis gas released from the wood.

Results

Wood/char heating

The simulated temperature profile in the wood cylinder, using 0.0 m/s inlet velocity, is depicted below. The measured wood centre temperature from Pyle and Zaror (1984) is also included. Figure 2 shows an excellent agreement between the simulated and the measured temperature at the centre of the wood particle.

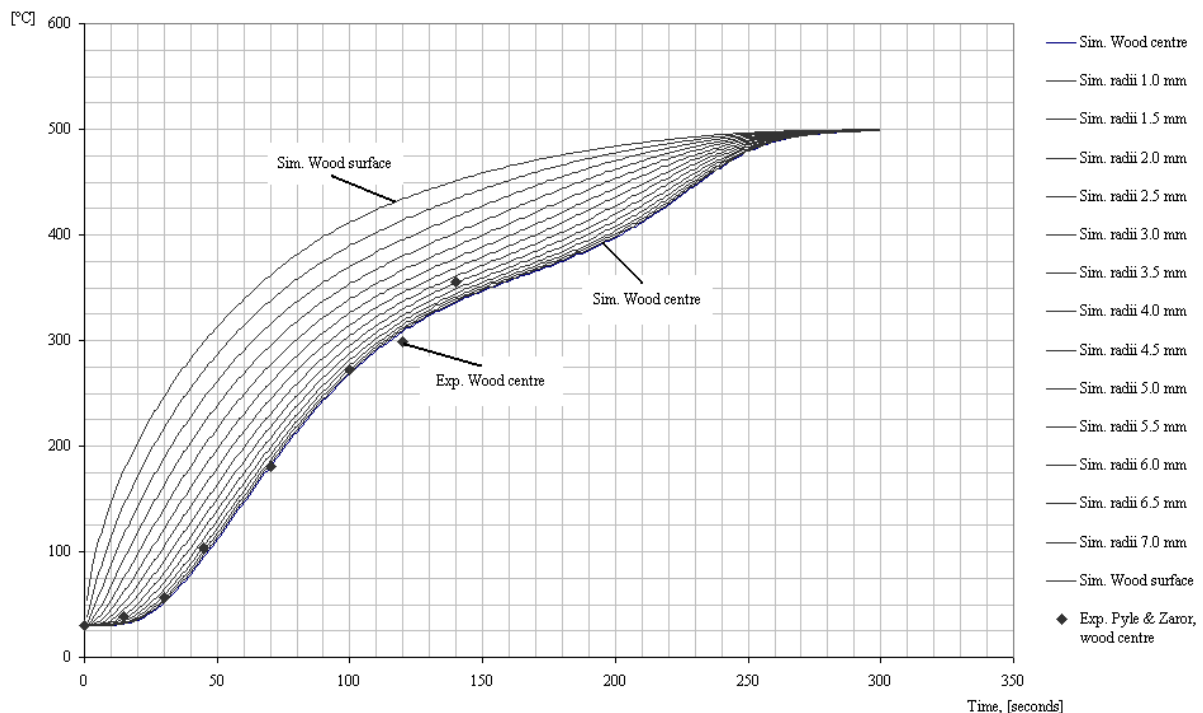


Figure 2: The temperature profile in the pine wood cylinder.

Rates of conversion

The simulated conversion and the measured conversion from Pyle and Zaror (1984) is depicted below. Comparing the simulation with the experiment, using an inlet velocity of 0.0 m/s, the simulation gives a result that is underestimating the conversion from wood to char at temperatures lower than 350 °C, and overestimates the conversion at temperatures in the region of 350 to 500 °C .

As pointed out by Pyle and Zaror (1984), the two most important factors for conversion is of course the wood temperature but also the activation energy since this is included in the influential exponential part of the Arrhenius pyrolysis rate.

Since the simulated wood centre temperature, shown in figure 2, agrees very well with the temperature measurements of Pyle and Zaror (1984), only erroneous rates of pyrolysis can explain the difference between the simulated and the measured conversion shown in figure 3. As shown in figure 3, the calculated conversion is within a reasonable range compared to the measurements, however there is a substantial difference between the gradients.

In order to achieve a better fit to the experimental data the activation energy and the pre exponential factor for the Arrhenius expression for the wood to char conversion needs to be altered. The activation energy should be lowered in order to reach an earlier conversion in the lower temperature region and the pre exponential factor must also be lowered somewhat to make the conversion slower in the higher temperature region.

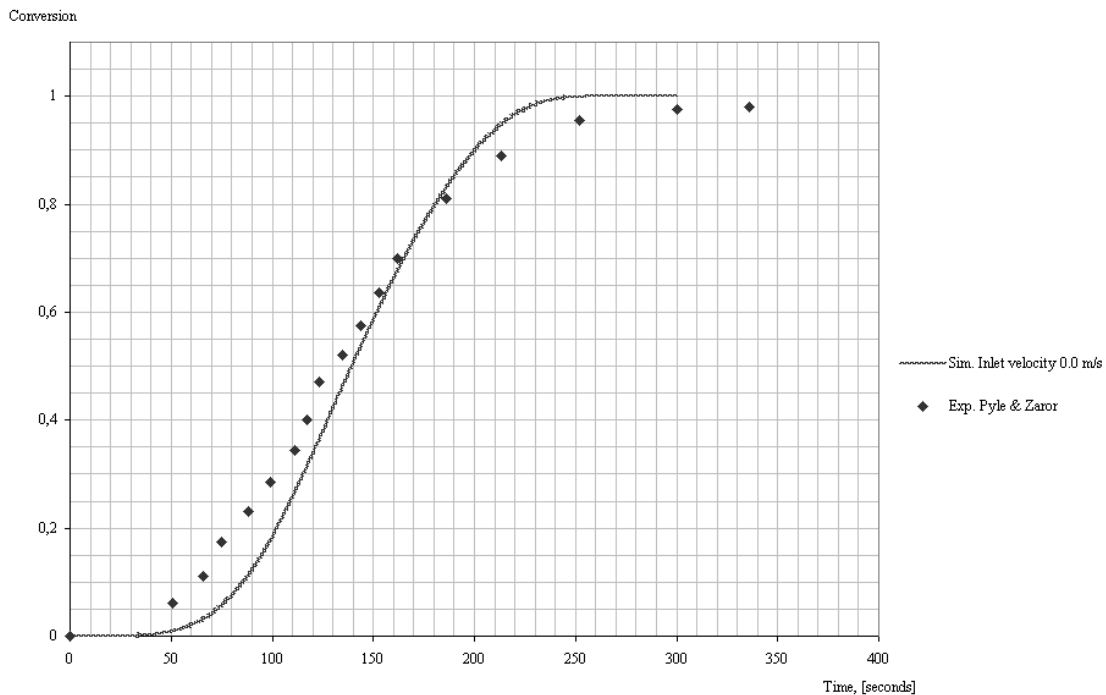


Figure 3: The history of conversion from wood to char.

Volatiles released to the surroundings

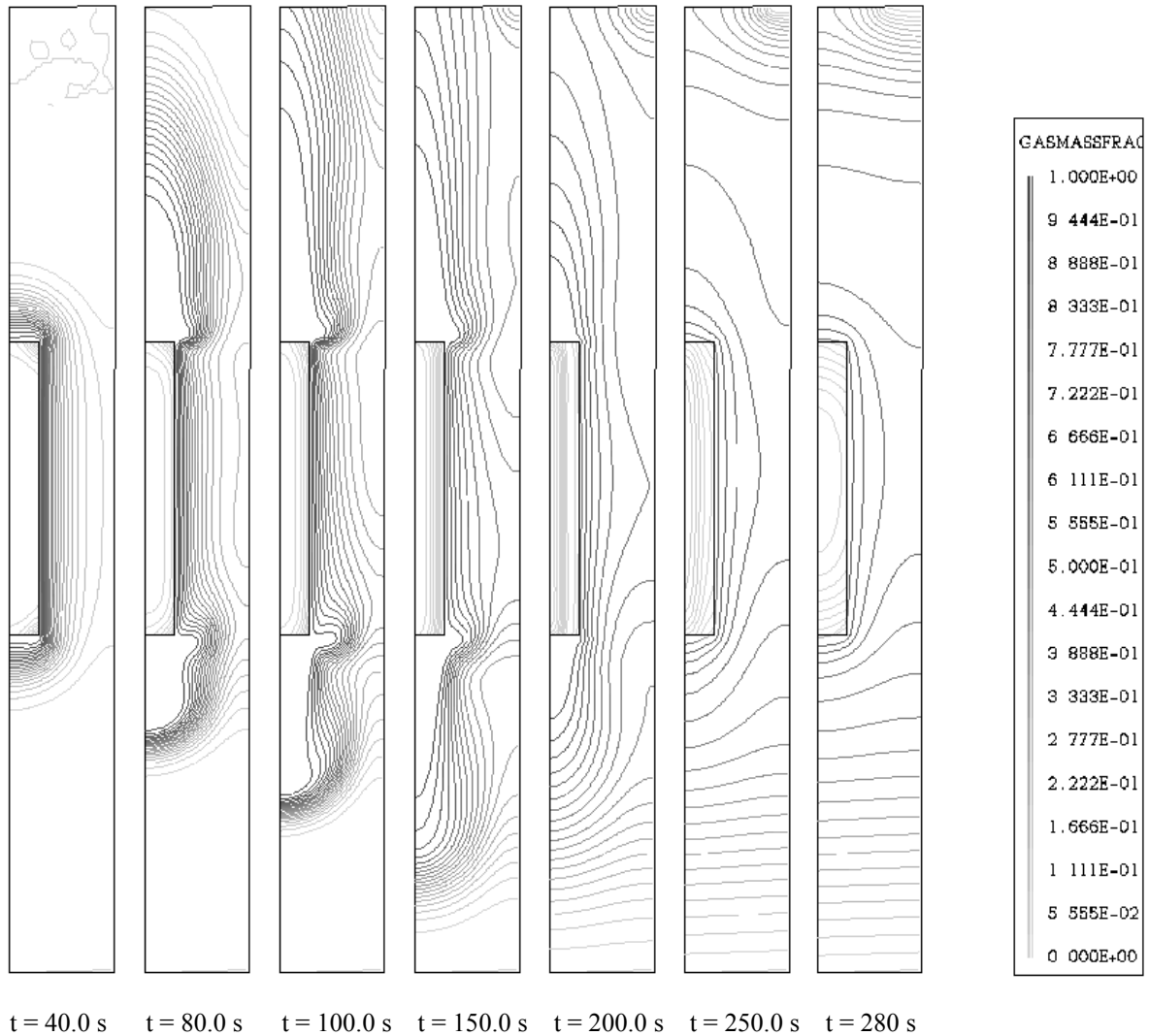


Figure 4: The distribution of the mass fraction of the released volatile pyrolysis gas at seven different time steps.

From the simulation it is possible to estimate the distribution of the mass fraction of the released volatile pyrolysis gas. As can be seen from figure 4, the production of the pyrolysis gas is initiated at approximately 40 s. At this stage the upper and lower corners are the most heated regions of the wood cylinder where already the pyrolysis process is initiated.

As the heating front progresses toward the centre of the wood cylinder, the production and release of the volatile gas is increasing. The gas plumes leaving the upper and lower wood ends have their maximum size at approximately 150 s. This coincides with the maximum conversion gradient at 150 s, as shown in figure 3. This therefore can be regarded as the point in time when the pyrolysis process is at its peak of reaction.

Between 150 s to 250 s, both the heating front and the pyrolysis front continues toward the wood cylinder centre and as shown in figure 3 the pyrolysis process diminishes gradually. At 250 s the temperature in the wood cylinder is almost uniform at 500 °C and the pyrolysis reaction has stopped since all the wood has been converted into char, tar and gas.

As we can see in figure 4, at 250 s the remaining pyrolysis gas in the wood cylinder migrates out of the wood and then at 280 s, the mass transport is mostly governed by diffusion.

From figure 5, it is possible to see the regions of higher momentum where the pyrolysis gas leaves the wood cylinder. As can be seen from the figures these regions are mainly at the wood cylinder upper and lower ends and coincide with the plumes of the mass fraction of the pyrolysis gas.

At 40 s, only the upper and lower wood cylinder corners are releasing small plumes of pyrolysis gas to the surrounding. The momentum of the plumes then increases and has moved halfway to the core of the wood cylinder at approximately 120 s. At 220 s the velocity plume is situated in the wood core and then at approximately 250 s, when the pyrolysis process has stopped, the velocity plume disappears.

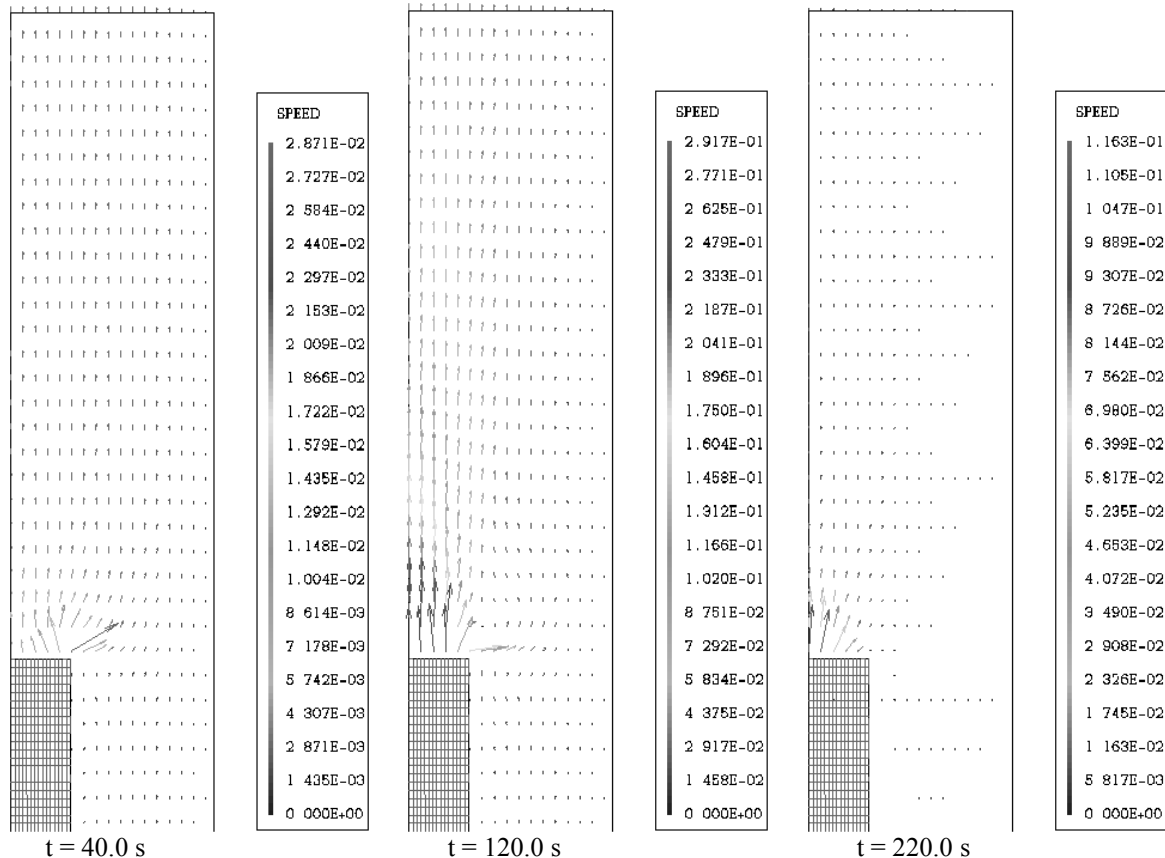


Figure 5: The velocity vectors for the volatile pyrolysis gas released out through the upper end surface of the wood cylinder, plotted for three different time steps.

Discussion

Permeability

When modelling the flow of the gas inside the wood/char pore structure one of the most important aspects is to use valid values of wood and char permeability. The permeability governs the direction of the flow in a porous media and it is often different in the radial, the tangential and the axial direction.

In the presented simulation the permeability of wood and char was taken from the work of Larfeldt (2000) and gives a solution for the flow field with plumes of pyrolysis gas migrating from the upper and lower ends of the wood cylinder. If, however the permeability would have been equal in all directions the migration of the pyrolysis gas would have taken place throughout all the outer area of the wood cylinder.

At present stage, the authors are unable to make any comparison with experimental data concerning the distribution of the concentration of produced pyrolysis gas and the speed by which it is transported.

Thermal conductivity

Numerous experiments have been presented on the topic of thermal conductivity of wood and char from wood and an extensive discussion on this topic can be found in the work by Grönli (1996). In the present work data for the thermal conductivity for wood and char was taken from the experimental work of Larfeldt (2000) where Larfeldt measured and modelled the thermal conductivity of birch wood and char from birch wood. One big difficulty is however to find experimental work on the data for thermal conductivity during the pyrolysis conversion from wood to char.

In the present work a model was implemented, based on discussions from Grönli (1996), which incorporates parallel and perpendicular heating where the different species thermal conductivity is weighted by the species volume fractions during the conversion.

Comparing the simulated temperatures with the measurements from Pyle and Zaror (1984), it is quite clear that the model for the thermal conductivity is giving good results, but the authors believe that more experimental and modelling investigations needs to be undertaken in order to fully understand the aspect of thermal conductivity during transition from wood to char.

Pyrolysis reaction rates

As mentioned earlier in this work the rate of conversion from wood to char, tar and gas has not been modelled fully in accordance with the data from the experiment of Pyle and Zaror (1984) and it is the authors opinion that a more suitable set of pyrolysis reaction rates should perhaps be used. However, from simulations using various reaction rates presented in literature, the authors believe that the reaction rates by Font et al. (1990), used in the present work, are the best yet available.

Thermodynamic and transport properties

The following set of thermodynamical and transport properties was used in the simulation. Some data was taken directly from Pyle and Zaror (1984) to give simulation results comparable with to the measurements from their experiments. The thermal conduction, the porosity and the permeability is from the work of Larfeldt (2000).

| Property: | Units: | Value: | Reference: |
|---|------------------------------------|-----------|----------------------------------|
| Wood density, ρ_w | [kg/m ³] | 550.0 | <i>Pyle and Zaror (1984)</i> |
| Char density, ρ_c | [kg/m ³] | 300.0 | <i>Pyle and Zaror (1984)</i> |
| Tar density, ρ_t | [kg/m ³] | 4.6821 | <i>Perry et al. (1997)</i> |
| Gas density, ρ_g | [kg/m ³] | 1.0396 | <i>Skreiberg et al. (1997)</i> |
| Wood conductivity, λ_w | [W/m K] | 0.2 | <i>Larfeldt (2000)</i> |
| Char conductivity, λ_c | [W/m K] | 0.09 | <i>Larfeldt (2000)</i> |
| Wood specific heat capacity, $C_{p,w}$ | [J/kg K] | 2439.0 | <i>Larfeldt (2000)</i> |
| Char specific heat capacity, $C_{p,c}$ | [J/kg K] | 1000.0 | <i>Larfeldt (2000)</i> |
| Tar specific heat capacity, $C_{p,t}$ | [J/kg K] | 1100.0 | <i>Janse et al. (2000)</i> |
| Gas specific heat capacity, $C_{p,g}$ | [J/kg K] | 1100.0 | <i>Di Blasi (1993a)</i> |
| Wood diffusivity, $D_{g,w}$ (gas in wood) | [m ² /s] | 1.0E-30 | <i>Estimated</i> |
| Char diffusivity, $D_{g,c}$ (gas in char) | [m ² /s] | 1.0E-30 | <i>Estimated</i> |
| Tar diffusivity, $D_{t,w}$ (gas in tar) | [m ² /s] | 1.0E-06 | <i>Chan et al (1985)</i> |
| Gas diffusivity, $D_{g,g}$ (volatiles in gas) | [m ² /s] | 0.148E-4 | <i>Perry et al. (1997)</i> |
| Wood porosity, ε_w | ----- | 0.68 | <i>Larfeldt (2000)</i> |
| Char porosity, ε_c | ----- | 0.9 | <i>Larfeldt (2000)</i> |
| Wood radial permeability, $\kappa_{w\perp}$ | [m ²] | 10.0E-14 | <i>Larfeldt (2000)</i> |
| Char radial permeability, $\kappa_{c\perp}$ | [m ²] | 10.0E-11 | <i>Larfeldt (2000)</i> |
| Wood axial permeability, $\kappa_{w\parallel}$ | [m ²] | 10.0E-10 | <i>Larfeldt (2000)</i> |
| Char axial permeability, $\kappa_{c\parallel}$ | [m ²] | 10.0E-8 | <i>Larfeldt (2000)</i> |
| Gas dynamic viscosity, μ_g | [kg/s m] | 3.0E-5 | <i>Larfeldt (2000)</i> |
| Wood emissivity, $\tilde{\varepsilon}_w$ | [W/m ² K ⁴] | 0.95 | <i>Koufopoulos et al. (1991)</i> |
| Char emissivity, $\tilde{\varepsilon}_c$ | [W/m ² K ⁴] | 0.75 | <i>Modest (1993)</i> |
| Wall emissivity, $\tilde{\varepsilon}_{wall}$ | [W/m ² K ⁴] | 0.35 | <i>Modest (1993)</i> |
| Stefan-Boltzmann constant, $\tilde{\sigma}$ | [W/m ² K ⁴] | 5.670E-8 | <i>Modest (1993)</i> |
| Heat of pyrolysis, $\Delta h_1 = \Delta h_2 = \Delta h_3$ | [J/kg] | -418000.0 | <i>Chan et al (1985)</i> |
| Heat of pyrolysis, $\Delta h_4 = \Delta h_5$ | [J/kg] | 42000.0 | <i>Koufopoulos et al. (1991)</i> |

Nomenclature

| Notation | |
|---------------|----------------------------------|
| A | Area |
| B | Body force |
| C_p | Specific heat |
| \bar{C}_p | Integrated average specific heat |
| \tilde{C}_p | Density weighted specific heat |
| D | Diffusivity |
| d | Diameter |
| H | Total enthalpy |
| h | Enthalpy |
| k | Rate of reaction |
| K | Area porosity |
| p | Pressure |
| Q | Energy source/sink term |
| R | Flow resistance |
| r | Species volume fraction |
| S | Mass source/sink term |
| T | Temperature |
| U | Velocity |
| Y | Species mass fraction |

| Greek letters | |
|-----------------------|------------------------------------|
| α, β | Specie |
| Δh | Heat of reaction |
| ε | Porosity |
| $\tilde{\varepsilon}$ | Emissivity |
| γ | Volume porosity |
| Γ | Diffusivity |
| κ | Permeability |
| λ | Thermal conductivity |
| φ | Volumetric shrinkage factor |
| μ | Viscosity |
| ρ | Density |
| σ | Stress tensor |
| $\tilde{\sigma}$ | Stefan-Boltzmann constant |
| ξ | Thermal conductivity bridge factor |
| Subscripts | |
| \perp | Perpendicular |
| \parallel | Parallel |
| eff | Effective value |

References

| |
|--|
| Di Blasi C., Modelling and simulation of combustion processes of charring and non-charring solid fuels, <i>Progr. Energy Combust. Sci.</i> , vol. 19, page 71-104, 1993. |
| Di Blasi C., Analysis of convection and secondary reaction effects within porous solid fuels undergoing pyrolysis, <i>Combust. Sci. and Tech.</i> , vol. 90, page 315-340, 1993. |
| Skreiberg Ö. et al., Kinetic NO _x modelling and experimental results from single wood particle combustion, <i>Fuel</i> , vol. 76, nr. 7, page 671-682, 1997. |
| Font R. Marcilla A. Verdu E. Devesa J., Kinetics of the pyrolysis of almond shells and almond shells impregnated with CoCl ₂ in a fluidised bed reactor and in a Pyroprobe 100, <i>Ind. Engng. Chem. Res.</i> , 29, page 1846-1855, 1990. |
| Liden A. G. Berruti F. Scott D. S., A kinetic model for the production of liquids from the flash pyrolysis of biomass, <i>Chem. Engng. Commun.</i> , 65, page 207-221, 1988. |
| Di Blasi C., Heat momentum and mass transport through a shrinking biomass particle exposed to thermal radiation, <i>Chemical engineering science</i> , vol. 51, nr. 7, page 1121-1132, 1996. |
| Koufopoulos C. A. et al., Modelling of the pyrolysis of biomass particles. Studies on kinetics, thermal and heat transfer effects, <i>The Canadian journal of chemical engineering</i> , vol. 69, page 907-915, August 1991. |
| Chan W-C. R. et al., Modelling and experimental verification of physical and chemical processes during pyrolysis of large a biomass particle, <i>Fuel</i> , vol. 64, page 1505-151, November 1985. |
| Larfeldt J. Leckner B. Melaen M. Chr., Modelling and measurements of drying and pyrolysis of large wood particles, <i>Fuel</i> , 79/13, 1637-1643, 2000. |
| Perry H. R. Green D. W., <i>Perry's chemical engineers'</i> , Platinum Edition, McGraw Hill, ISBN 0-07-135540-5, 1999. |
| Modest M. F., <i>Radiative heat transfer</i> , McGraw Hill, ISBN 0-07-112742-9, 1993. |
| Janse A. M. C. Westerhout R. W. J. Prins W., Modelling of flash pyrolysis of a single wood particle, <i>Chemical engineering and processing</i> , 39, 239-252, 2000. |
| Grønli M., A theoretical and experimental study of the thermal degradation of biomass, Ph-D thesis, NTNU Norges teknisk-naturvitenskaplige Universitet, 1996. |
| Pyle D. L. Zaror C. A., Heat transfer and kinetics in the low temperature pyrolysis of solids, <i>Chem. Eng. Sci.</i> , vol. 39, 147-158, 1984. |
| Davidsson K. O. Pettersson J. B. C., Birch wood particle shrinkage during rapid pyrolysis, <i>Fuel</i> , 81, 263-270, 2002. |